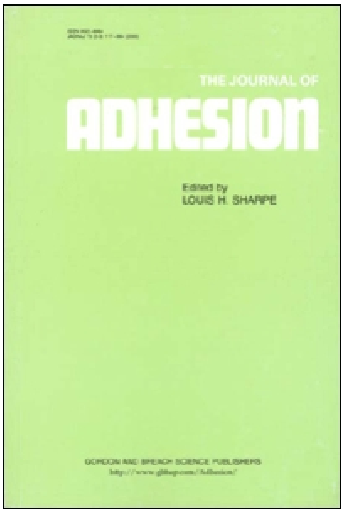

The Journal of Adhesion
Publication details, including instructions for authors and subscription information:
http://www.informaworld.com/smpp/title~content=t713453635

Direct Measurement of Energy Barriers on Rough and Heterogeneous Solid Surfaces

Thomas B. Lloyd[a]; Guy M. Connelly[b]
[a] Polymer Interface Center, Lehigh University, Bethlehem, PA, USA [b] Connelly Applied Research, Nazareth, PA, USA

To cite this Article Lloyd, Thomas B. and Connelly, Guy M.(1997) 'Direct Measurement of Energy Barriers on Rough and Heterogeneous Solid Surfaces', The Journal of Adhesion, 63: 1, 141 — 157
To link to this Article: DOI: 10.1080/00218469708015218
URL: http://dx.doi.org/10.1080/00218469708015218

J. Adhesion, 1997, Vol. 63, pp. 141–157
Reprints available directly from the publisher
Photocopying permitted by license only

Direct Measurement of Energy Barriers on Rough and Heterogeneous Solid Surfaces*

THOMAS B. LLOYD[a,**] and GUY M. CONNELLY[b]

[a]*Polymer Interface Center, Lehigh University, Bethlehem, PA 18015, USA;*
[b]*Connelly Applied Research, Nazareth, PA 18064, USA*

(Received 30 October 1995; In final form 12 July 1996)

The "three-liquid" contact angle approach to the surface free energy components of solids was applied to poly (vinyl fluoride), rough and flattened, with and without flame treatment. Lifshitz-van der Waals (LW), γ_{SL}^{LW}, and acid-base (AB), γ_{SL}^{LW}, components were determined and used to calculate $-\Delta G_{SL}$ ($W_{SL}^{adhesion}$) for the formation of interfaces of five liquids with polymer. The automated goniometer allowed the determination of the energy barriers, $-\Delta G_{SL}^{*}$ as the advancing liquid moved from pinned configuration to a metastable one. The acid-base component of the barriers was much greater than the LW, and the magnitude of the barriers was only slightly reduced by flattening.

Keywords: Liquid-solid adhesion; contact angle; energy barriers to wetting; acid-base parameters; Lifshitz-van der Waals forces; hysteresis

INTRODUCTION

Professor Good has long been involved in the use of contact angles to characterize surfaces and interfaces. Fairly recently Good, Chaudhury and van Oss introduced a combining rule for electron acceptor-donor interactions, including those across interfaces [1]. Quantification of this hypothesis is proceeding, and this work is a part of it. Specifically, the

---

*One of a Collection of papers honoring Robert J. Good, the recipient in February 1996 of *The Adhesion Society Award for Excellence in Adhesion Science, sponsored by 3M.*

**Corresponding author.

research here was aimed at characterizing poly (vinyl fluoride) relative to the adhesion of aqueous inks.

This paper will deal with the phenomenon of energy barriers to the spreading of liquids on solids. These barriers often manifest themselves as a "pinning" of a sessile drop as liquid is very slowly added to it. That is, the volume of the drop increases, but the interfacial diameter does not. Thus, the advancing contact angle (θ_a) increases to a maximum. At the point where the hydrostatic pressure in the drop overcomes the "pinning" force the diameter suddenly increases (jumps), and the drop relaxes to a metastable configuration which has a lower θ_a (see Fig. 1). The outward flow continues until the three-phase line encounters the next barrier capable of arresting the flow. This phenomenon has been seen by many workers. Adam and Jessop [2] proposed a frictional force which would oppose the advancement of the liquid. They were interested in applying the idea to contact angle hysteresis and abandoned the approach. Schwartz *et al.* [3] addressed the issue of resistance to flow in capillary systems, measuring the minimum pressure needed to induce flow, defined as the critical line force. They refer to measurements (by others) of this "pinning" force by movement of drops down an inclined plane, movement of liquids in capillaries under air pressure and by a dipping plate.

A number of investigators have applied geometrical calculations to the spreading of liquids on rough surfaces and have raised the issue of

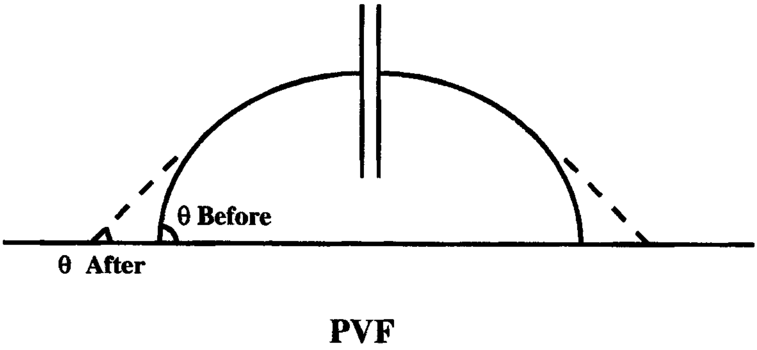

FIGURE 1 Sessile drop going from maximum angle, θ^{before}, and returing to the lower metastable angle, θ^{after}.

energy barriers [4, 5, 6, 7]. Johnson and Dettre [8, 9] deal theoretically with idealized rough surfaces and experimentally with low-energy surfaces of varying roughness. None, to our knowledge, have taken a direct approach to the measurement of the energy barriers such as we use here using static "recently advanced" angles. Shanahan [10] develops a model (no experimental data) for the "stick-slip" behavior of receding angles where triple-line jumps have been observed on evaporating sessile drops. Here the drop volume change is very slow, and he assumes that the angle reached immediately after the jump is described by Young's equation. We will discuss below the implications of our experimental procedure on the definition of our "energy barriers".

Energy barriers should be considered in many applications such as the spreading of liquid adhesives where thorough wetting is the goal. The interfacial forces involved are of both the Lifshitz-van der Waals (LW) and acid-base (AB) type [1]. Also, surface roughness plays a role. We will describe how we measure the energy barriers on real surfaces directly and resolve them into their LW and AB components.

THEORY

The work of adhesion for the formation of a solid-liquid interface can be expressed as the sum of the works of adhesion due to LW and to AB attractive forces, presuming no electrostatic interaction [1]:

$$W_{SL}^{Total} = W_{SL}^{LW} + W_{SL}^{AB} \qquad (1)$$

and $W_{SL}^{Total} = -\Delta G_{SL}$, the free energy change upon forming the interface. W_{SL}^{LW} is twice the geometric mean of the LW components of the cohesive free energies of the solid and the liquid, or:

$$W_{SL}^{LW} = 2(\Upsilon_S^{LW}\Upsilon_L^{LW})^{1/2} \qquad (2)$$

The total work of adhesion can be established *via* the Young-Dupré equation and the contact angle:

$$W_{SL}^{Total} = \Upsilon_L(1 + \mathrm{Cos}\theta) \qquad (3)$$

If an apolar liquid, *i.e.* $\Upsilon_L^{AB} = 0$, of known Υ_L^{LW} (diiodomethane in this case) is used on the solid, Equation (3) becomes $W_{SL}^{LW} = \Upsilon_L^{LW}(1 + \cos\theta)$ which allows the determination of Υ_S^{LW} by using Equation (2) [11].

Knowing W_{SL}^{LW} and applying Equations (1) and (3) with any liquid yields W_{SL}^{AB}. Here, we have used the series of liquids described by Good, Chaudhury and van Oss in their "three-liquid" approach to quantizing the acidic and basic nature of surface sites on solids [12]. In this procedure, the acidic contribution to the cohesive surface tension (Υ_L^+) of the liquids and the basic contribution (Υ_L^-) were established [13]. These values are then used in their new interfacial combining rule:

$$W_{SL}^{AB} = 2(\Upsilon_S^+ \Upsilon_L^-)^{1/2} + 2(\Upsilon_S^- \Upsilon_L^+)^{1/2} \tag{4}$$

Reference 12 gives the values of Υ_L^+ and Υ_L^- for the liquids used here: diiodomethane (liquid #1 for W_{SL}^{LW}), water (liquid #2) used in combination with a third liquid to establish W_{SL}^{AB}. Since Υ_S^+ and Υ_S^- are unknown, two equations are needed to solve Equation (4) [12]. That is, an equation for water and one for another pure polar liquid are used. We used water in conjunction with glycerol, ethylene glycol and formamide, respectively.

W_{SL}^{AB} can be arrived at by using Equations (1), (2), and (3), as well as by using Equation (4). Equation (4) gave values of W_{SL}^{AB} identical to those from the approach using Equations (1), (2) and (3) for water on all the surfaces described below.

However, for the other three polar liquids Equation (4) gave slightly lower W_{SL}^{AB} values. Also, the values of Υ_S^+ and Υ_S^- give insight into the nature of the active sites on the poly (vinyl fluoride) samples of varying chemical activity and roughness that were used in the experiment. Keep in mind that these are not "ideal" surfaces.

Using this approach and measuring the contact angle at its maximum "before" unpinning and at its lower metastable "after" configuration, we can calculate the free energy difference between the two. This is the height of the "energy barrier" as we define it here $(-\Delta G_{SL}^*)$. Further, with the proper choice of liquids, we can resolve the total free energy into its LW and AB components.

The procedure for determining the maximum and metastable angles is described immediately below. Since liquid is pumped into the drop there may be an inertial effect which would cause an "unpinning" before the maximum θ was reached. To minimize this, we set a slow flow rate, consistent with gathering a large number of θ's in each situation, for statistical purposes. The flow pattern of the incoming liquid, however, as seen when particles were introduced for demonstration, tended to curl upward and away from the three-phase line. Whereas we may be underestimating the barriers, we regard our values as a close approach but further work on refining the procedure would be helpful.

EXPERIMENTAL MATERIALS AND PROCEDURES

Poly (vinyl fluoride), DuPont's Tedlar®, extruded film was used in three forms: clear (unpigmented); pigmented with titanium dioxide, which imparts surface roughness; and the latter flame-treated commercially. All were aged about a year and, therefore, were at a steady state. The film was washed with methanol and acetone to remove residual dimethyl acetamide used as an aid to extrusion. These three surfaces were expected to differ in chemical activity, since the flame-treated material is designed to improved the adhesion of coatings applied to it.

Samples of the films were further modified by flattening, as follows. The two virgin films were pressed against glass at 150°C and 17.2 MPa (2,500 psi) for 10 minutes, resulting in glossy surfaces. The flame-treated film could not be removed from the glass after this procedure; therefore, the clear PVF was used as a release film. Glossy surfaces were not achieved even at 160°C and 27.6 Mpa (4,000 psi); therefore, the flamed, flattened surface was not as smooth as the virgin, flattened surface. Flattening the unpigmented (clear) film appeared to have little effect, since it was already quite flat, but it did become more glossy.

Figure 2 shows the considerable flattening done on the pigmented virgin film. XPS showed that the flame-treated PVF surface was 30.2 at. % F as compared with 33.5 at. % for the virgin, and flaming increased the oxygen content from 2.3 to 4.5 at. %. Flattening had little chemical effect on the flamed film (where a release film was used); however, the virgin sample when flattened (against glass) dropped in F to 31.0 at. % the oxygen rose to 3.4 at. % and Si went from

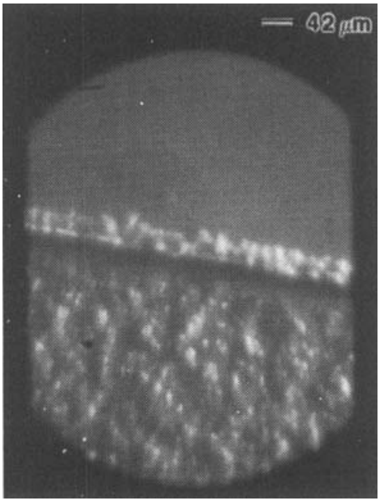

FIGURE 2 Pigmented virgin Tedler (PVF) before (bottom) and after (top) flattening (120x).

0 to 0.9 at. %. Obviously, flattening against glass contaminated the surface with glass, and this was noted in the contact angle measurements.

The computer driven goniometer (Connelly Applied Research, Nazareth, PA, USA) instrument slowly establishes a liquid sessile drop of about 5 mm diameter on the film in an environmental chamber. The volume is ~10–30 µl, depending on θ. Liquid was then pumped at ~0.5 µl/sec using a computer-controlled syringe pump to add to and later to take from the drop. Maximum volume was ~40–120 µl. Video images from the long-range microscope were recorded at ~45/min and then digitized. As the liquid advanced from one metastable configuration to the next in discontinuous fashion, an optical trigger mechanism, which checked for motion 30 times/second, stopped the pump at the onset of the "jump" and retained the maximum θ_a just before the advance. After one minute the image at the next configuration was recorded. These images were labeled "before" (maximum θ_a) and "after" (metastable θ_a). Contact angles were established on both sides of the profile of the drop using a sub-pixel interpolation method. The data were stored and calculations of Υ_S^+ and Υ_S^- were overdetermined in a matrix of all possible pairs of the polar liquids.

Drop diameter ranged from 4.5 to 7.6 mm to avoid any influence of size on θ_a. We could discern no pattern of the measured angles, or their differences, which would indicate declining inertial effects, as the diameter was increased. This gave us confidence that such inertial effects were small.

An average of thirty (fifteen left/right) $\theta_a^{before} - \theta_a^{after}$ measurements were made on each surface with each liquid. The differences in the means were t-tested and found to differ, as expected *i.e.* "before" higher, with a high degree of confidence, averaging 97.8% for the polar liquids, and ~91% for diiodomethane. This variation was the statistical issue most critical to this work. The differences of $\theta_a^{before} - \theta_a^{after}$ ranged from 1.0° to 2.9° for the polar liquids (with possible outliers at 0.5° and 6.1°) on the various surfaces. Diiodomethane ranged only $-0.5° \pm 0.9°$. Reproducibility was estimated statistically for three drops of water on rough, flamed PVF. These data are typical of the polar liquids. Each drop was advanced six times. The estimate of repeatability, drop to drop, was 1.11°; reproducibility was estimated at 1.09° and precision at 1.56°.

Since receding angles often tended to decrease as the diameter of the drop was reduced sequentially, usually only the first recession was used in the hysteresis calculation. We do not know the reason for this behavior, but it may be due to the time that the liquid has been in contact with the surface. However, where subsequent recessions gave a constant θ_r, two or three were averaged. Note that the receding angle is measured after the three-phase line has retreated. Thus, it may differ from the θ_r measured on a tilted plate [9].

The diiodomethane (99%, Aldrich) was purified through a column of alumina, stored over copper turnings, and stored in the dark. The water was distilled and glycerol (99%, Aldrich), ethylene glycol (certified, Fisher) and formamide (98%, Aldrich) were used as received.

RESULTS AND DISCUSSION

Table Ia shows the three Υ_s parameters which were calculated from contact angles as described above. Note (as an illustration) the effect of helium plasma treatment on the unpigmented PVF. The plasma increased all three Υ_s values and no roughening was seen by atomic

TABLE Ia Υ_s Parameters for PVF*

	Using ADVANCING θ						*Using RECEDING θ*		
	Before (maximum)			*After (final)*			*After (final)*		
Unpigmented virgin	Υ_s^{LW}	Υ_s^+	Υ_s^-	Υ_s^{LW}	Υ_s^+	Υ_s^-	Υ_s^{LW}	Υ_s^+	Υ_s^-
As received	36.0	0.11	5.7	36.1	0.18	6.1	41.1	0.33	8.5
Flat	33.5	0.07	3.9	33.5	0.14	4.3	42.0	0.06	8.7
Plasma treated	----	----	----	42.4	0.45	21.5	----	----	----
Pigmented Virgin									
As received (rough)	36.5	0.40	2.1	36.7	0.48	2.7	45.0	0.67	24.2
Flat	35.9	0.06	14.3	36.0	0.15	13.6	44.1	0.25	21.6
Pigmented Virgin, Flame treated									
As received (rough)	38.5	0.19	4.1	38.9	0.29	4.6	46.9	0.41	31.5
Flat	30.4	0.38	17.1	30.4	0.52	17.7	44.5	0.38	38.8

*overdetermined values for Υ_s^+ and Υ_s^- (3 pairs of polar liquids).

force microscopy. The Υ_S^+ values are lower and Υ_S^- higher for the unpigmented than for the as-received pigmented virgin. Since these samples were produced by DuPont at different times, these differences were not surprising. However, the small change in acidity (Υ_S^+), and increase in basicity (Υ_S^-), due to flaming of the as-received films, appears to be real.

To give an idea of the variability involved in the experiments, the standard errors of θ for the polar liquid pair, water/ethylene glycol (EG), were propagated to Υ_S^+, Υ_S^- and W_{SL}^{AB}. This was done for pigmented PVF surfaces of least standard deviation (σ) in θ (virgin-rough) and where the greatest σ's were encountered (flamed-flat). The results are given in Table Ib.

It can be seen that the "before" results were slightly less variable on the virgin-rough but more variable on the flamed-flat. The standard errors of W_{SL}^{AB} for EG averaged slightly less than for water. However, since the work terms were lower, the percent standard error is higher for EG.

In all cases, the values of W_{SL}^{AB} were positive (Tab. II) when calculated by the combining rule, Equation (4), as well as by the use of Equations (1), (2) and (3) shown in brackets. Perhaps more importantly, the energy barriers, are all positive as well although they are small differences in ("after"–"before") work of adhesion (Tab. III). Thus, the precision of the measurements allowed establishment of the proper sign of the barrier in all cases.

TABLE Ib Illustration of Parameters (mJ/m^2) with Errors Propagated from Contact Angles*

	Virgin-Rough		*Flamed-Flat*	
	"After"	*"Before"*	*"After"*	*"Before"*
Υ_s^+	0.97 ± 0.01	0.91 ± 0.009	0.36 ± 0.045	0.23 ± 0.11
Υ_s^-	2.0 ± 0.08	1.37 ± 0.036	18.8 ± 0.21	18.3 ± 0.26
W_{SL}^{AB}				
Ethylene Glycol	17.4 ± 1.1	16.3 ± 0.71	20.2 ± 1.6	18.4 ± 2.6
Water	24.3 ± 1.2	21.5 ± 0.48	49.8 ± 2.6	48.0 ± 3.1

*For polar liquid pair, water/ethylene glycol.

Note : Values in the other Tables are the result of combining three polar liquid pairs.

The reasons for the changes due to flattening are not readily apparent and suggest the need for attention to this point in the "three liquid" approach. However, the effect was consistent, "before" and "after", and presented a consistent energy barrier picture. We suspect that the large increase in basicity (Υ_S^-) was due to an increase in the concentration of basic sites, as the real area under the drop was reduced by flattening. The effect this had on Υ_S^+ followed Υ_S^- for the flamed but not the virgin film, probably because of the glass contamination of the virgin material.

The Υ_S^+ and Υ_S^- values in Table Ia were used in Equation (4) to determine the work of adhesion due to acid-base interfacial forces of the liquids on the six PVF surfaces. Values are given in Table II. In Figures 3a and 3b, Υ_L^{Total} values are plotted of the four polar liquids *versus* W_{SL}^{AB} (or $-\Delta G_{SL}^{AB}$). Even though there is scatter in the data, in all cases the W_{SL}^{AB} "before" values are lower than the "after". That is, the liquids spread spontaneously to the metastable configuration from the top of the energy barriers. Errors propagated to W_{SL}^{AB} through Equation (4) for selected cases are given in Table Ib.

TABLE II Comparison of W_{SL}^{AB}(mJ/m^2) for the Polar Liquids as Calculated by Equation (4) versus Equations (1, 2, 3)

using Advancing θ "before" and Equation (4) and in brackets by [Eqs. (1,2,3)]

Pigmented Tedlar Film	*Water*	*Glycerol*	*Ethylene Glycol*	*Formamide*
Virgin Rough	21.0 [21.5]	15.3 [7.2]	12.7 [17.1]	12.3 [19.3]
Flat	40.7 [40.8]	18.7 [16.5]	13.8 [14.2]	14.5 [15.7]
Flamed Rough	24.8 [25.8]	14.6 [2.6]	11.6 [17.7]	11.6 [18.8]
Flat	48.0 [48.2]	25.7 [22.7]	19.9 [18.4]	20.2 [24.8]

using Advancing θ "after" and Equation (4) and in brackets by [Eqs. (1,2,3)]

Pigmented Tedlar Film	*Water*	*Glycerol*	*Ethylene Glycol*	*Formamide*
Virgin Rough	23.6 [24.2]	17.0 [8.7]	14.1 [17.3]	13.7 [20.0]
Flat	41.2 [41.5]	20.5 [19.6]	15.5 [16.0]	16.0 [19.6]
Flame Rough	27.1 [27.6]	16.7 [3.4]	13.3 [18.3]	13.3 [22.4]
Flat	49.8 [49.7]	27.6 [24.0]	21.5 [20.3]	21.8 [26.8]

TABLE III Energy Barriers, $-\Delta G^*_{SL} = (-\Delta G^{after}_{SL}) - (-\Delta G^{before}_{SL})$, to spreading of Liquids (mJ/m^2)

				Unpigmented Virgin		*Pigmented Virgin*		*Pigmented Virgin-Flame treated*	
PVF	*Liquid*	γ_L^{LW}	γ_L^{AB}	*LW*	*AB*	*LW*	*AB*	*LW*	*AB*
As Rec'd	DIM	50.8	0	0.1	0	0.3	0	0.5	0
Flat				0	0	0.1	0	0	0
Ac Rec'd	Water	21.8	51.0	0.1	1.7	0.2	2.6†[a]	0.6	2.3
Flat				0	2.1	0	0.5	0	1.8[c]
As Rec'd	Glycerol	34	30	0.1	1.7	1.0	1.7	0.3	2.0
Flat				0	2.1	0	1.8	0	1.9
As Rec'd	Formamide	39	19	---	---	0.2	1.3	0.4	1.7
Flat				---	---	0.1	1.5	0	1.5
As Rec'd	Ethylene Glycol	29	19	1.6	1.5	0.9	1.4[b]	0.4	1.7
Flat				0	1.8	0.1	1.7	0	1.6[d]
As Rec'd	Average of all			0.48	1.63*	0.52	1.75*	0.44	1.93*
Flat				0	2.00*	0.06	1.38*	0	1.70*

*DIM not included in average.

†see text for comment on standard error.

[a] ± 1.2; [b] ± 1.3; [c] ± 4.0; [d] ± 3.0.

Figure 3a relates the W_{SL}^{AB} of the polar liquids on pigmented virgin PVF, rough and flattened. The reason for the higher values for flattening was commented upon above. Note also that flattening increased W_{SL}^{AB} more with rising surface tension of the liquids. When the surface was flamed, we see the same trends (Fig. 3b). Comparing Figures 3a and 3b we see that the rough surfaces are essentially equal in W_{SL}^{AB}. However, when the surfaces were flattened, the effect of flaming was seen. That is, flattening increased W_{SL}^{AB} on an average $33 \pm 8\%$ for the four polar liquids. A tentative conclusion is that topography dominates on the rough surfaces, especially here where the chemical changes were not great.

Figure 4 relates the Υ_L^{LW} of the five liquids to their W_{SL}^{LW} on the same surfaces as in Figures 3a and 3b. In this figure only the "after" θ_a values were used in calculating W_{SL}^{LW}, because "before" and "after" angles were essentially equal. That is, the Lifshitz-van der Waals for-

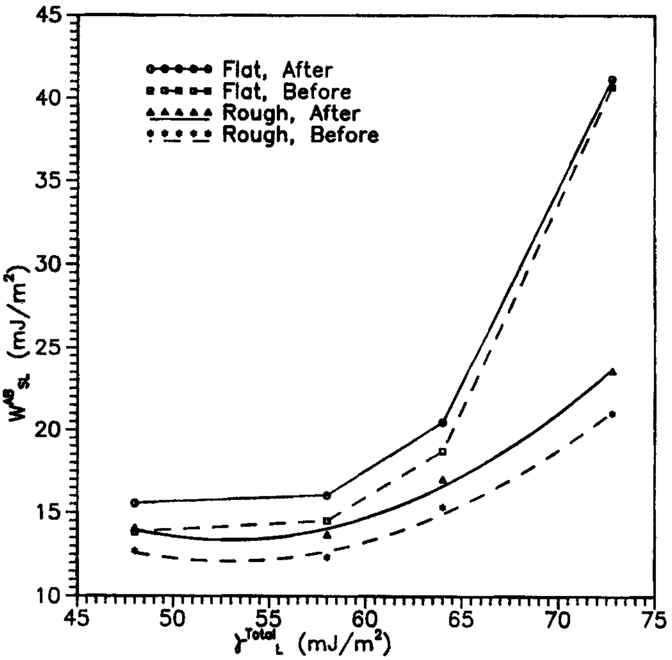

FIGURE 3a Υ_L^{Total} *vs* W_{SL}^{AB} using Eq. (4) for pigmented virgin PVF.

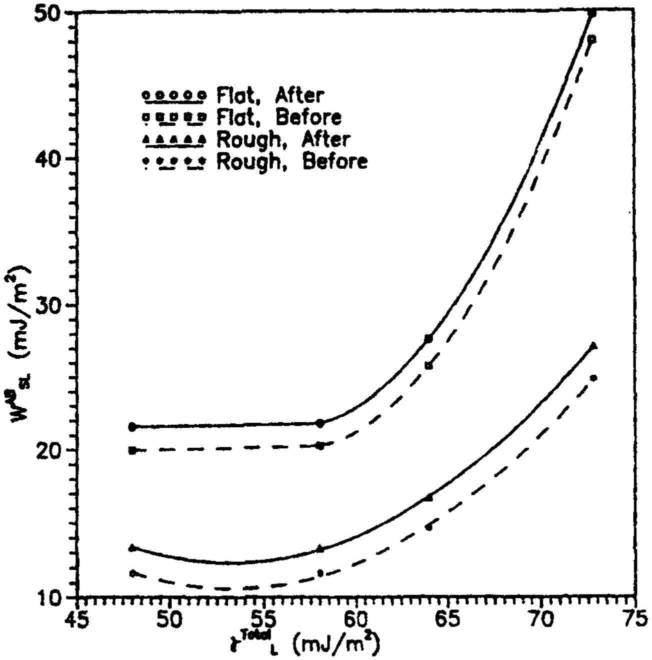

FIGURE 3b Υ_L^{Total} *vs* W_{SL}^{AB}, using Eq. (4) for flame-treated, pigmented PVF.

ces did not contribute much to the energy barriers (see below). The W_{SL}^{LW} correlates very strongly with Υ_L^{LW}, the linear coefficient being essentially 1.0 in each case. The following observations can be made:

1. Flattening the rough virgin film lowered W_{SL}^{LW} by only $1.0 \pm 0.6\%$, while the flamed film was lowered $11.6 \pm 0.1\%$. This very large difference could not be a roughness (surface area) effect because a very much smaller effect was seen with the virgin film which was not flamed. Rather it is a consequence of the low Υ_S^{LW} of the flamed, flat film, i.e. a high θ_a with diiodomethane. Possibly that film was contaminated but for whatever reason, the energy barrier was not influenced, as seen in the next section.
2. Comparing Figure 4 with 3a and 3b: $W_{SL}^{LW} \succ W_{SL}^{AB}$.

W_{SL}^{AB} values were calculated using Equations (1), (2) and (3) for the four pigmented film surfaces (as plotted in Figs. 3a and 3b) and com-

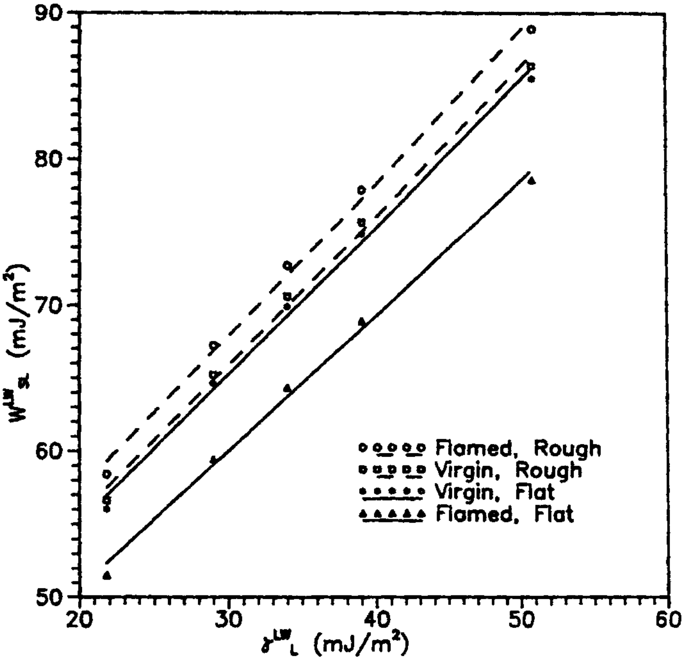

FIGURE 4 Υ_L^{LW} *vs* W_{SL}^{LW}, using Eq. (2) for rough and flat, virgin flamed PVF.

pared with Equation (4) values in Table II. The two procedures for W_{SL}^{AB} gave almost identical results for water on all surfaces. In the case of glycerol the rough surfaces gave low values using Equations (1), (2) and (3), probably because this high viscosity liquid trapped air as it spread, giving a composite surface. This effect was diminished in the matrix used to calculate Υ_S^+ and Υ_S^- for use in Equation (4). Eliminating the glycerol data for the rough surfaces, the average percent difference in W_{SL}^{AB} as calculated by the two approaches (based on Equation (4) values) was 9% for the flat surfaces and 30% for the rough. Thus, the Equation (4) approach is validated for flat surfaces. Indeed the Equation (1), (2) and (3) calculation of W_{SL}^{AB} would have given more scatter in all the Figures 3a and 3b curves had they been plotted. These curves where plotted with W_{SL}^{AB} values calculated *via* Equation (4) only.

Energy Barriers

Table III shows the energy barriers in terms of free energy change calculated (using Equation (4) for W_{SL}^{AB}) for the various liquids spreading on the solids. In the case of the LW interfacial force, the barrier is almost nil on the flat surfaces and averages only 0.6% of their $-\Delta G_{SL}^{LW}$ (or W_{SL}^{LW}) on the rough, as-received. The energy barriers due to the acid-base forces were much higher than the LW and did not appear to be influenced by roughness. On average, the AB energy barriers were slightly higher for rough virgin and flamed, than for the flattened ones. In terms of relationship to $-\Delta G_{SL}^{AB}$, virgin and flamed AB barriers were equal at $10.6 \pm 0.4\%$ of their $-\Delta G_{SL}^{AB}$. On flattened surfaces these AB barriers were again equal at $5.8 \pm 0.1\%$ of their $-\Delta G_{SL}^{AB}$.

The values in Table III are small and the standard error was not propagated to these values of Υ_S^+, Υ_S^- through the overdetermined matrix.

However, using one liquid pair (water and ethylene glycol) on two surfaces, we propagated the error to the values shown in Table III. Whereas one might expect a few calculated free energy changes to be positive due to statistical fluctuation, in every case ΔG_{SL} was negative for the "jumps".

Although there are only a few data points, the acid-base component of the barrier correlates well with Υ_L^{AB}. The linear correlation coefficients for the rough surfaces are: pigmented virgin (1.0), flamed (0.99). On flattened surfaces the correlation is poorer. If Υ_L^{Total} is used, we again see a lesser correlation. Thus, we see that the energy barriers are essentially acid-base in character and their magnitude is little influenced by roughness.

Hysteresis

Table IV lists the hysteresis for the liquids on the several surfaces. In general, flattening decreased hysteresis as expected. Exceptions to this were DIM and formamide on the flamed pigmented PVC and ethylene glycol on pigmented virgin as well as on flamed. These liquids are the ones of lower surface tension, but hysteresis does not correlate well with the surface tension of the liquids, either Υ_L^{Total} or Υ_L^{AB}.

TABLE IV Hysteresis ("After") = $\theta_a - \theta_{rec}$

PVF	*Liquid*	*Unpigmented Virgin*	*Pigmented Virgin*	*Pigmented virgin-Flame treated*
As received	DIM	12.8	29.4	19.0
Flat		9.4	16.7	27.6
As received	Water	8.9	33.9	37.0
Flat		11.0	14.8	29.6
As received	Glycerol	10.2	40.1	46.9
Flat		10.9	15.0	37.1
As received	Formamide	---	25.2	16.0
Flat		---	15.1	22.0
As received	Ethylene Glycol	14.7	14.3	16.7
Flat		9.9	21.6	20.5
As received	Average (all liquids)	11.7 ± 2.6	28.6 ± 9.7	27.1 ± 14.0
Flat		10.3 ± 0.8	16.6 ± 2.9	27.4 ± 6.6

We thought that there might be a relationship between the energy barriers and hysteresis, but none was found.

Note the average hysteresis of all the liquids, first on the flat surfaces (bottom line, Tab. IV). As the chemical heterogeneity increases so does the hysteresis as well as its range. On the "as-received" surfaces we see the same trend, but the first step to the right is greater because of the added increase in roughness. It is interesting that as greater chemical heterogeneity is added by flaming the hysteresis does not change. Therefore, these two sources of hysteresis are not additive. Note also that the rough surfaces have a greater range of hysteresis than the flat. The behavior of the low Υ_L liquids (DIM, formamide and ethylene glycol) is responsible for this and more work is needed before drawing a firm conclusion.

CONCLUSION

An automated goniometer capable of measuring the maximum contact angle of a spreading sessile drop allows the calculation of the energy barriers encountered. Using the "three-liquid" approach to resolve the barriers into their LW and AB components, the latter were found to be dominant. The AB barriers were 10.6% of $-\Delta G_{SL}^{AB}$ for rough PVF surfaces and 5.8% for the same surfaces after flattening. The LW barriers were only 0.6% of $-\Delta G_{SL}^{LW}$ on rough surfaces and nil on flat.

The magnitude of the energy barriers were not related to roughness, in general, although $-\Delta G_{SL}^{AB}$ was increased by flattening.

The acid-base work of adhesion as determined by the three-liquid approach is very close to the values calculated from $W_{SL}^{AB} = W_{SL}^{Total} - W_{SL}^{LW}$ when applied to flat surfaces.

No relationship between energy barriers and hysteresis was found. For virgin PVF the hysteresis was greater on the rough than on the flat surface. However, on the more active flamed surface only, water and glycerol (higher Υ_L) showed more hysteresis for the rough.

Acknowledgements

The authors greatly appreciate the finanical support of the Boeing Airplane Co., the valuable advice of Prof. James E. Sturm, the XPS analyses by David A. Cole of Evans East and the laboratory work of Kathleen (Ferretti) Theodorou.

References

[1] Van Oss, C. J., Chaudhury, M. K. and Good, R. J., *Chem. Rev.* **88**, 927 (1988).
[2] Adam, N. K. and Jessop, G., *J. Chem. Soc.* **127**, 1863 (1925).
[3] Schwartz, A. M., Rader, C. A. and Huey, E., *Advances in Chemistry Series 43* (Amer. Chem. Soc. Washington, DC, 1963), Chap. 17.
[4] Shuttleworth, R. and Bailey, G. L. J., *Disc. Faraday Soc.* **3**, 16 (1948).
[5] Bikerman, J. J., *J. Phys. Chem.* **54**, 653 (1950).
[6] Good, R. J., *J. Amer. Chem. Soc.* **74**, 5041 (1952).
[7] Schwartz, A. M. and Minor, F. W., *J. Colloid Sci.* **14**, 584 (1959).
[8] Johnson, R. E., Jr. and Dettre, R. H., *Advances in Chemistry Series 43* (Amer. Chem. Soc., Waghington, DC, 1963), Chaps. 7 and 8.
[9] Johnson, R. E., Jr. and Dettre, R. H., in *Surface and Colliod Sci.*, Matijevic, E., Ed. (1969), Vol. 2, p. 85.
[10] Shanahan, M. E. R., *Langmuir* **11**, 1041 (1995).
[11] Fowker, F. M., *Surface and Interfacial Aspects of Biomedical Polymers*, Andrade, J. D., Ed. (Plenum, New York, 1985), Vol. 1, Chap. 9.
[12] Good, R. J., *J. Adhesion Sci. Technol.* **6**, 1269 (1992).
[13] Van Oss, C. J., Good, R. J. and Busscher, H. J., *J. Dispersion Sci. Technol.* **11**(1), 75 (1990).